AIP | Journal of Applied Physics

Thermal growth and structural and optical characterization of indium tin oxide nanopyramids, nanoislands, and tubes

D. Maestre, A. Cremades, J. Piqueras, and L. Gregoratti

Citation: J. Appl. Phys. **103**, 093531 (2008); doi: 10.1063/1.2919770
View online: http://dx.doi.org/10.1063/1.2919770
View Table of Contents: http://jap.aip.org/resource/1/JAPIAU/v103/i9
Published by the American Institute of Physics.

Thermal growth and structural and optical characterization of indium tin oxide nanopyramids, nanoislands, and tubes

D. Maestre,[1,a)] A. Cremades,[1] J. Piqueras,[1,b)] and L. Gregoratti[2]
[1]*Departamento de Física de Materiales, Facultad de Ciencias Físicas, Universidad Complutense de Madrid, 28040 Madrid, Spain*
[2]*Sincrotrone Trieste, Area Science Park, 34012 Basovizza-Trieste, Italy*

(Received 11 February 2008; accepted 7 March 2008; published online 12 May 2008)

In-doped SnO_2 microtubes as well as Sn-doped In_2O_3 (ITO) nano- and microislands have been grown by thermal treatment of compacted SnO_2–In_2O_3 powders under argon flow at 1350 °C in a catalyst-free process. The SnO_2 tubes contain about 1 at. % of In, even when the In content in the starting mixture was as high as 52 at. %. However, the ITO nanoislands and nanopyramids, grown preferentially on the faces and edges of the tubes, present an In content up to six times higher than the tubes. Spatially resolved cathodoluminescence shows a higher emission from the Sn-rich structures, so that the In-rich ITO nanoislands show dark contrast in the CL images. CL spectra show that the main emission bands in both, Sn-rich and In-rich, structures, are related to oxygen deficiency. X-ray photoelectron spectroscopy shows differences between the tubes and the nanoislands in the O $(1s)$ spectral region. In particular, a component at 531.9 eV of the O $(1s)$ signal appears enhanced in the In-rich islands. © *2008 American Institute of Physics*.
[DOI: 10.1063/1.2919770]

I. INTRODUCTION

Tin-doped indium oxide (ITO) is a transparent conductor which has attracted interest due to its applications in fields such as display devices, solar cells, or gas sensing. ITO films for these and other applications are normally produced by different methods and their properties have been often investigated. As in the case of other semiconductor oxides, there is an increasing interest in one-dimensional nanostructures of SnO_2, In_2O_3, as well as of In-doped SnO_2 and Sn-doped In_2O_3, with potential applications in nanotechnology. In particular, tin-doped indium oxide nanowires have been grown by a carbon-assisted technique,[1] a co-precipitation-annealing process[2] and vapor-liquid-solid thermal processes.[3–6] Also, a thermal evaporation process has been used to synthesize indium-doped tin oxide nanowires.[7] In the present work, ITO nano- and microstructures have been grown by thermal treatment of compacted mixtures of SnO_2 and In_2O_3 powders, with different weight ratios, under argon flow. This method has been previously reported to lead to the growth of elongated structures of different semiconductor oxides on the surface of the sample, so that neither a catalyst nor a foreign substrate is used.[8–13] In Ref. 8, the growth of SnO_2 micro- and nanotubes with rectangular cross section was reported, while in the case of In_2O_3,[11] wires, necklace- and arrow-shape structures were grown from InN.

The investigation of the growth behavior and properties of these nano- and microstructures is considered to be a crucial step toward the functionalization of different nano- and microdevices.

In this work, different ITO structures are obtained, whose morphology and composition depend on the composition of the starting mixture. The structures have been characterized by x-ray diffraction (XRD), scanning electron microscopy (SEM), cathodoluminescence (CL) in SEM, x-ray energy dispersive spectroscopy in SEM and x-ray photoelectron spectroscopy (XPS).

II. EXPERIMENTAL SECTION

The starting materials used were commercial SnO_2 powder of 99.9% purity and In_2O_3 powder of 99.997% purity. Mixtures of both powders with SnO_2:In_2O_3 weight ratios of 2:1, 1:1, 1:2, 1:10, and 1:30, respectively, were prepared by milling the powders in a centrifugal ball mill, Retsch S100, with 20 mm agatha balls for 5 h. Disk shaped samples of about 7 mm diameter and 2 mm thickness were fabricated by compacting the milled powders under a compressive load. The samples were then annealed at 1350 °C for 10 h in a furnace under argon flow. Hereinafter, the samples will be labeled with the mentioned weight ratios in the initial mixtures used to prepare them (2:1, 1:1, 1:2, 1:10, and 1:30).

XRD measurements were performed in a Philips diffractometer. The samples were observed in the secondary electron and CL modes in a Hitachi S-2500 or a Leica 440 SEM at beam voltages in the range of 10–30 kV at 80 K. For the CL images, a Hamamatsu R-928 photomultiplier was used and the CL spectra were recorded either with an Oriel 78215 monochromator or with a Hamamatsu PMA-11 charge coupled device camera. Spatially resolved XPS measurements were performed at the ESCA microscopy beamline of the Elettra synchrotron facility in Trieste. Photoemission spectra were measured with a spot size of about 150 nm, 500 eV photon energy, and 0.2 eV energy resolution which allows us to probe the core level chemical shifts.

[a)]Electronic mail: davidmaestre@fis.ucm.es.
[b)]Author to whom correspondence should be addressed. Electronic mail: piqueras@fis.ucm.es.

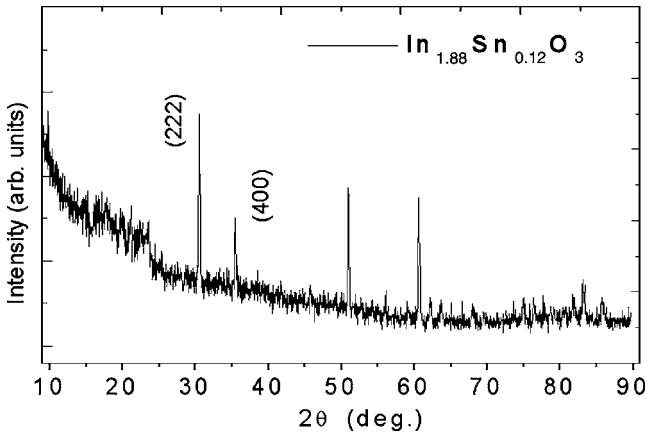

FIG. 1. XRD spectrum of sample 1:1, showing the peaks that can be indexed as $In_{1.88}Sn_{0.12}O_3$.

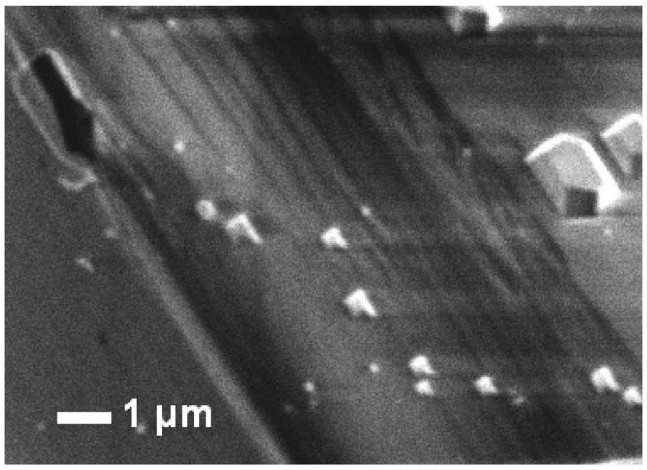

FIG. 3. Image of a group of islands with different sizes grown on the face of a tube.

III. RESULTS AND DISCUSSION

XRD shows that the initial milled mixture consists of SnO_2 and In_2O_3 but does not contain an ITO phase, while the presence of ITO is only detected in the thermal treated samples. Figure 1 shows the XRD spectrum of the annealed sample 1:1, whose main peaks can be assigned to the compound $In_{1.88}Sn_{0.12}O_3$. Similar XRD spectra are also observed in samples fabricated with different initial mixtures. The presence of the (222) and (400) peaks in the XRD curves of the annealed samples indicates the formation of ITO during the thermal treatment.

In the samples with a high tin oxide fraction in the initial powder, namely, 2:1, 1:1 and 1:2, tubular structures with rectangular cross section grow on the sample surface. Their number increases with the SnO_2 content, so that in the 2:1 sample, the surface is practically covered by the structures. Figures 2(a) and 2(b) show one large tube and a group of tubes, respectively, grown in this sample. Nano- and microislands, some of them with triangular pyramidal shapes, are observed on the faces of the tubes. In Fig. 2(a), arrays of islands appear along the edges of the tube opening and along the internal edges, which seem to be favorable nucleation sites. Figure 2(c) shows a distribution of islands and Fig. 2(d) shows one pyramid. Some pyramids can be also observed on the tubes of Fig. 2(b). As Fig. 2(c) shows, the islands tend to align parallel to the edge of the tubes and to the growth ridges which are often observed in the faces.

Figure 3 shows a region of a face containing islands with sizes ranging from about 100 nm to the micron range. In samples fabricated with tin oxide–indium oxide ratios of 1:10 and 1:30, no tubes are observed so that these samples will not be considered in the following discussion.

EDX measurements performed in different points of the surface of the sample grown with oxides ratio 1:1, agree with the presence of the ITO compound $In_{1.88}Sn_{0.12}O_3$ detected by

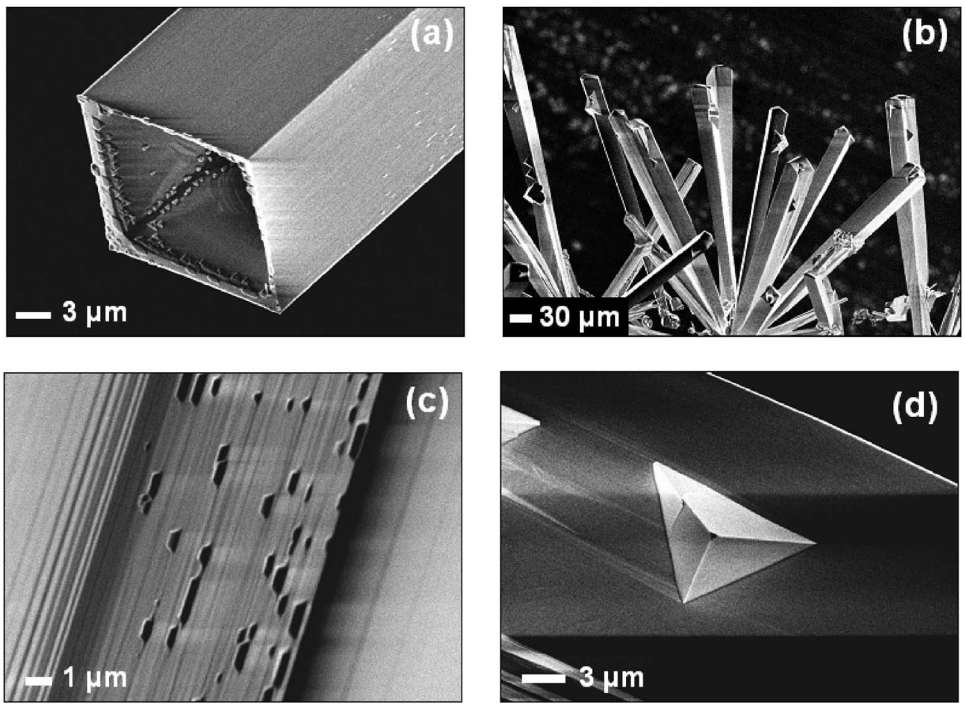

FIG. 2. Tube (a) and a group of tubular structures (b), grown on sample 2:1. A distribution of micro- and nanoislands (c) and a pyramidal shape island (d) grown on the faces of the tubes.

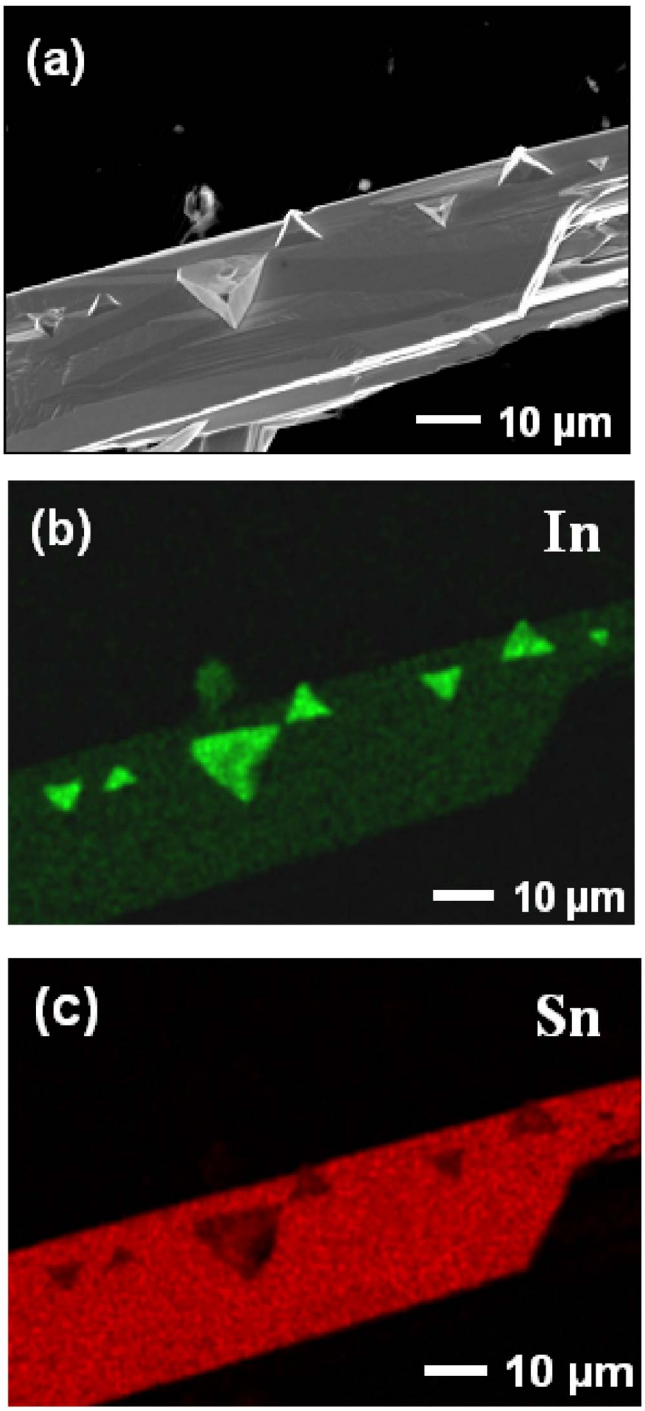

FIG. 4. (Color online) EDX compositional maps of In (b) and Sn (c) acquired on the tube shown in (a).

XRD. The at. % composition of this compound is In (37.6%), Sn (2.4%), and O (60%) which is close to that detected by EDX, e.g., In (35.9%), Sn (2.4%), and O (61.7%). However, the composition of the tubes and the islands were found to be different from that of the surface of the sample. The atomic In content in the faces of the tubes was found to be about 1% of the Sn content, while the typical compositional values in the islands reveal that In at. % is higher than that of Sn by a factor of about 6. This shows that the tubes consist of In doped SnO_2 and the islands grown on their faces consist of Sn doped In_2O_3. Figures 4(b) and 4(c) show In and Sn EDX maps acquired on the tube observed in Fig. 4(a), revealing the enhanced amount of In in the islands as compared to the rest of the tube.

Rectangular SnO_2 tubes have been previously grown by the same thermal method described here, when pure SnO_2 powder was used as precursor.[8] As discussed in Ref. 8, the most probable growth direction of the tubes is [101] and the narrow and wide lateral surfaces of the rectangular tube would be the (010) and (10−1) planes, respectively. The present results show that the growth of the tubes, with morphology related to the SnO_2 tetragonal structure, takes place only when the starting mixture contains a high fraction of SnO_2, at least the 1:2 ratio. During the growth process, only a small fraction of the In atoms is incorporated into the tubular structures, while the rest condensates to form the In-rich islands.

The formation of nano- and microstructures with different amounts of In and Sn influences the luminescence behavior of the samples. Figure 5(a) shows the normalized CL spectra of the powders used in the starting mixture. A broad-band peaked at about 1.94 eV and a weaker band at about 2.58 eV are observed in the CL spectrum of SnO_2, while the spectrum of In_2O_3 shows a band at 1.84 eV. In the treated samples, the luminescence from the tubes is considerably more intense than the emission from the surface of the compacted pellet on which the tubes grow. Figure 5(b) shows the spectra recorded, respectively, in the surface and in the tubes of sample 2:1. Both spectra are similar to that of pure SnO_2 powder, with a main band at about 1.96 eV. The spectrum of the surface also shows a weak band at about 2.58 eV, as well as a weak emission extending to higher energies. By increasing the amount of In_2O_3 in the initial mixture, the relative CL emission of the high energy luminescence of the tubes increases. The shift of CL luminescence to higher energies by increasing the indium oxide content is apparent in Fig. 5(c) which shows the spectra from samples 2:1 and 1:30. Since sample 1:30 does not contain tubes, in this case, the spectra correspond to the surfaces of both samples.

A CL band at 1.94 eV has been previously reported for sintered SnO_2 powders and for rectangular undoped SnO_2 tubes, grown by the same procedure used in this work, and has been attributed to oxygen vacancy related centers.[8,14] Since the tubes grown in this work contain only about 1 at. % of In, we suggest that the CL emission from the tubes [Fig. 5(b)], arises mainly from oxygen vacancy defects in the SnO_2 lattice as in the undoped tubes. The presence of these defects causes a higher luminescence from the tubes as compared to the sample surface. CL emission close to 2.58 eV has been reported for SnO_2 and In_2O_3 structures, which indicates that the weak band at this energy shown in Fig. 5(b) is probably related to both oxides. Increasing the amount of In_2O_3 leads to spectra in which the 1.96 eV band of SnO_2 is not dominant, as Fig. 5(c) shows. CL emission at about 1.90 eV also appears in In_2O_3 nanostructures.[11] Luminescence at 1.90–2 eV has been reported for Sn-doped In_2O_3 films[15] and In-doped SnO_2 nanowires[7] and attributed to oxygen deficiency and surface states, respectively.

The fact that CL spectra and CL intensity depend on the Sn:In ratio and that the Sn rich structures are more lumines-

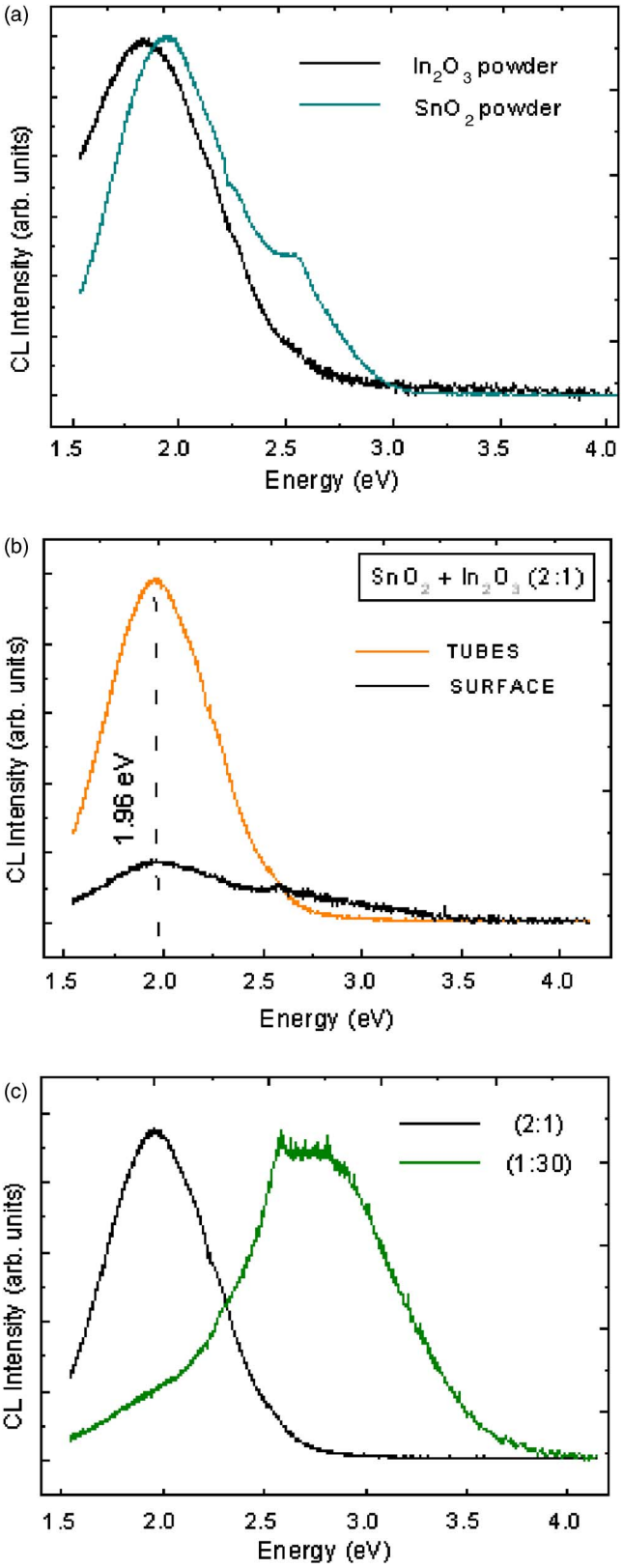

FIG. 5. (Color online) (a) Normalized CL spectra of the initial SnO_2 and In_2O_3 powders. (b) CL spectra of the surface and the tubes grown on sample 2:1. (c) Normalized CL spectra of samples 2:1 and 1:30.

cent, is also apparent in the CL images as those of Fig. 6 which show a tube of the 2:1 sample. It is observed that the face of the tube emits with higher intensity than the In-rich islands, which appear with a dark contrast. As shown in Figs.

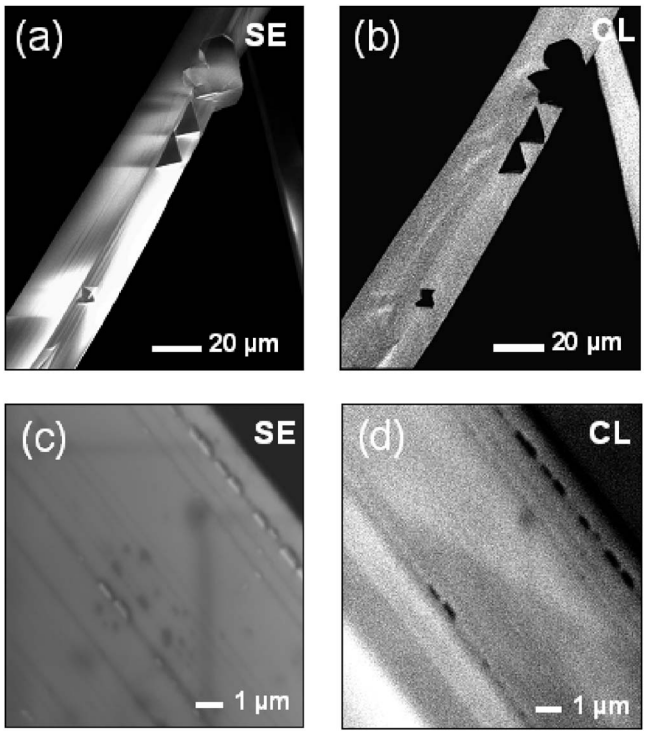

FIG. 6. SEM images of the pyramidal islands (a) and nanoislands (c) grown on a tube, as well as the respective cathodoluminescence images [(b) and (d)].

6(b) and 6(d), both small and pyramidal islands present a similar behavior. The tubes show an enhanced CL emission from their inner part as has been previously observed in undoped SnO_2 tubes,[8] which is related to the characteristic distribution of defects.

Figure 7 shows a region of the XPS spectrum of the starting mixture used to prepare sample 2:1, where the O (1*s*), In (3*d*), and Sn (3*d*) core levels peaks can be observed. In this case, the positions of the peaks were calibrated with respect to the C (1*s*) peak (284.6 eV) from the residual carbon.

The quantification of the integrated areas of the XPS curves reveals changes in the atomic In/Sn ratio after the

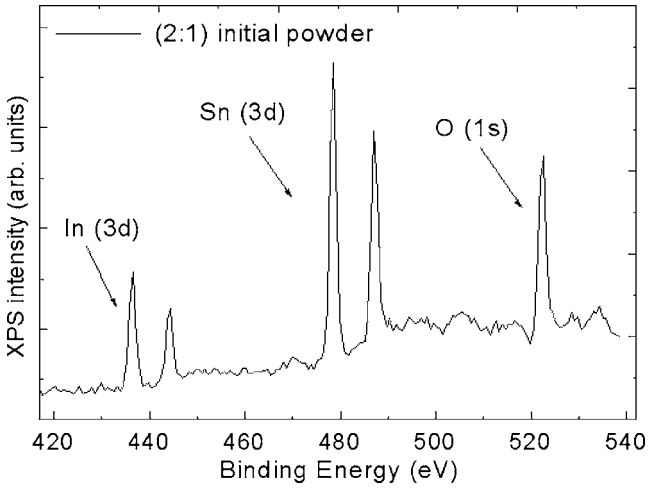

FIG. 7. XPS spectrum of the initial mixture of powders used in the fabrication of sample 2:1, showing the In (3*d*), Sn (3*d*), and O (1*s*) core levels.

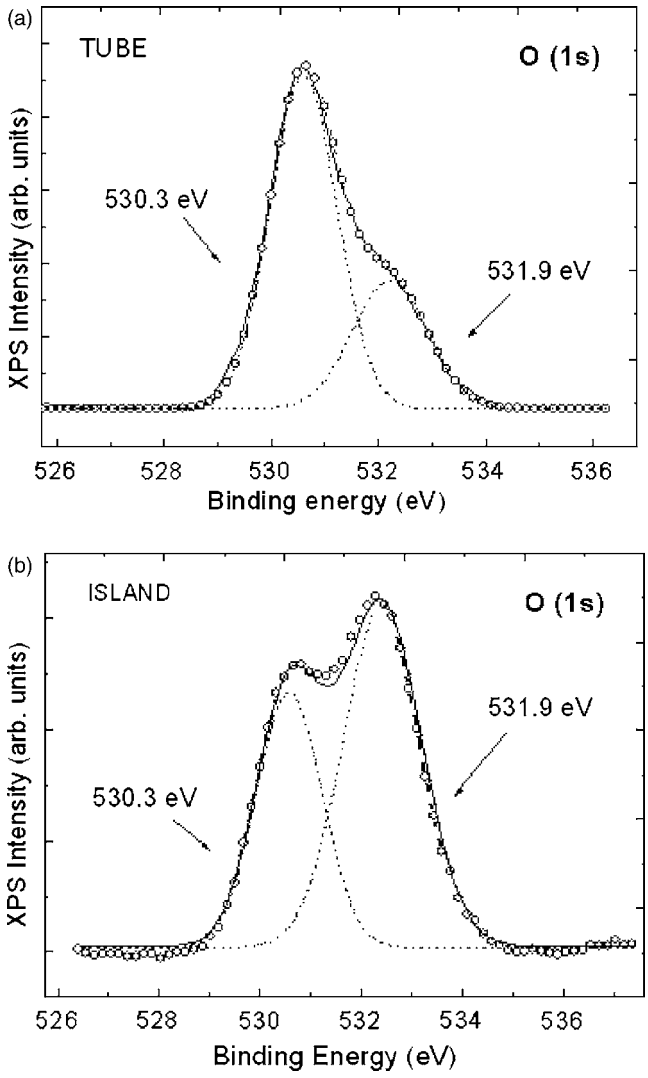

FIG. 8. XPS spectra of the O (1*s*) core level and a deconvolution showing two components, acquired on the lateral face (a) and an island (b) of a tube grown on sample 2:1.

thermal treatments. The study of the XPS spectra recorded on the surface of the annealed samples concludes that an increase in the In/Sn ratio occurs after the thermal treatment. The obtained In/Sn values for the precursor powders 2:1 and 1:1 are 0.38 and 1.18, respectively, while XPS spectra recorded on regions without tubes of the annealed samples surface, show that the thermal treatment causes an increase in the In/Sn values up to 4.72 (sample 2:1) and 5.35 (sample 1:1). This effect is associated with a decrease in the Sn content on the surface of the samples, which would be compensated by the growth of the Sn-rich tubes. Local XPS measurements performed on the tubes and the islands, show that the tubes are formed by In-doped SnO_2 while the islands grown on the faces of the tubes consist of Sn-doped In_2O_3, which confirms the EDX and CL results. Regardless the composition of the initial mixture, the tubes present typical In/Sn values of 0.5–0.7, while there is a higher variation of the In/Sn values for the islands, ranging from 4 to 7. These results cannot be quantitatively compared with the composition measured by EDX due to the different nature, surface or bulk in the micron range, of the techniques. XPS reveals a higher In at. % on the surface of the tubes than the value measured by EDX. The XPS spectra show binding energies of 444.8 eV for In (3*d*), 486.9 eV for Sn (3*d*) and two values, 530.3 and 531.9 eV for O (1*s*), in agreement with previously reported results in different indium tin oxide systems.[2,5,16,17] The relative intensities of the two O (1*s*) components depend on the region probed, being the 531.9 eV component more intense in regions with high In concentration. This is shown in the XPS spectra of Fig. 8, corresponding to the O (1*s*) region recorded on a tube face and on an island, respectively. The 530.3 eV peak has been attributed to oxygen in crystalline ITO or In_2O_3 (Refs. 16, 18, and 19) and the high energy peak has been related to amorphous In_2O_3 (Refs. 16 and 19) or to oxygen deficient regions of ITO. The enhanced 531.9 eV signal would indicate a marked oxygen deficiency in the surface of the ITO islands.

IV. CONCLUSIONS

Sintering of SnO_2–In_2O_3 compacted mixtures under argon flow leads to the growth of In-doped SnO_2 microtubes, with rectangular cross section, and Sn-doped In_2O_3 nano- and microislands. The ITO islands grow on the faces and edges of the microtubes. XRD and EDX measurements show that the Sn-rich microtubes, which contain about 1 at. %. In, grow during sintering of the compacted mixture leaving an In-rich substrate. The In at. % in the ITO islands is about six times higher that the Sn at. %. CL imaging from tubes and islands show a higher emission from the Sn-rich structures or regions while CL spectra show that the main luminescence bands in Sn-rich and In-rich structures correspond to oxygen deficiency. Spatially resolved XPS measurements show an enhancement of the high energy component at 531.9 eV of the O (1*s*) signal, in the In-rich islands.

ACKNOWLEDGMENTS

This work was supported by MEC (Project No. MAT2006-01259).

[1]K. P. Kalyanikutty, G. Gundiah, C. Edem, A. Govindaraj, and C. N. R. Rao, Chem. Phys. Lett. **408**, 389 (2005).
[2]D. Yu, D. Wang, W. Yu, and Y. Qian, Mater. Lett. **58**, 84 (2004).
[3]Y. Q. Chen, J. Jiang, W. Wang, and J. G. Hou, J. Phys. D **37**, 3319 (2004).
[4]Q. Wan, Z. T. Song, S. L. Feng, and T. H. Wang, Appl. Phys. Lett. **85**, 4759 (2004).
[5]S. Y. Li, C. Y. Lee, P. Lin, and T. Y. Tseng, Nanotechnology **16**, 451 (2005).
[6]Q. Wan, P. Feng, and T. H. Wang, Appl. Phys. Lett. **89**, 123102 (2006).
[7]X. Y. Xue, Y. J. Chen, Y. G. Liu, S. L. Shi, Y. G. Wang, and T. H. Wang, Appl. Phys. Lett. **88**, 201907 (2006).
[8]D. Maestre, A. Cremades, and J. Piqueras, J. Appl. Phys. **97**, 044316 (2005).
[9]E. Nogales, B. Méndez, and J. Piqueras, Appl. Phys. Lett. **86**, 113112 (2005).
[10]J. Grym, P. Fernández, and J. Piqueras, Nanotechnology **16**, 931 (2005).
[11]D. A. Magdas, A. Cremades, and J. Piqueras, Appl. Phys. Lett. **88**, 113107 (2006).
[12]P. Hidalgo, B. Méndez, and J. Piqueras, Nanotechnology **18**, 155203 (2007).
[13]Y. Ortega, P. Fernández, and J. Piqueras, Nanotechnology **18**, 115606 (2007).
[14]D. Maestre, A. Cremades, and J. Piqueras, J. Appl. Phys. **95**, 3027 (2004).
[15]A. El Hichou, A. Kachouane, J. L. Bubendorff, M. Addou, J. Rbothe, M. Troyon, and A. Bougrine, Thin Solid Films **458**, 263 (2004).

[16]Y. S. Kim, Y. C. Park, S. G. Ansari, B. S. Lee, and H. S. Shin, Thin Solid Films **426**, 124 (2003).
[17]M. Yamaguchi, A. Ide-Ektessabi, H. Nomura, and N. Yasui, Thin Solid Films **447–448**, 115 (2004).
[18]R. X. Wang, C. D. Beling, S. Fung, A. B. Djurisic, C. C. Ling, and S. Li, J. Appl. Phys. **97**, 033504 (2005).
[19]N. Mori, S. Ooki, N. Masubuchi, A. Tanaka, M. Kogoma, and T. Ito, Thin Solid Films **411**, 6 (2002).